*The 2017 World Congress on*
***Advances in Structural Engineering and Mechanics (ASEM17)***
*28 August - 1 September, 2017, Ilsan(Seoul), Korea*

# Hydrogen-assisted cracking in super duplex stainless steel characterized by scanning probe microscopy

*Bai An and Takashi Iijima

*National Institute of Advanced Industrial Science and Technology (AIST)*
*Tsukuba, Ibaraki 305-8569, Japan*
*b.an@aist.go.jp*

## ABSTRACT

Understanding the hydrogen-assisted cracking in multiphase steels is of scientific and engineering importance. A combination of scanning electron microscopy (SEM) and scanning probe microscopy (SPM) is applied to investigate the micromorphology of fracture surface and microcrack formation in hydrogen-precharged super duplex stainless steel. Hydrogen precharging was performed in gaseous hydrogen under 138 MPa pressure at 573 K and slow strain tensile testing was performed at room temperature in air. It is observed that the fracture surface consists of quasi-brittle facets, which exhibit small dimplelike patterns or quasi-periodic corrugation patterns at the nanoscale. The hydrogen-assisted microcracks preferentially initiate and grow in ferrite phase and are stopped or deflected by the boundaries of the austenite phase. The hydrogen-assisted cracking mechanisms in duplex stainless steel are discussed on the base of the experimental results and hydrogen-enhanced localized plasticity theory.

## 1. INTRODUCTION

Duplex stainless steels consisting of austenite (γ) and ferrite (α) provide excellent combination of mechanical properties and corrosion resistance, and thus have been widely used in the oil and gas, petrochemical, paper and nuclear industries. However, their very favorable properties are degraded due to hydrogen embrittlement (HE) (Marrow 1991, Zheng 1991). The microscopic analysis of hydrogen-induced cracking in duplex stainless steels have shown that hydrogen-induced microcracks often start and grow in the ferrite phase and can be arrested in the austenite phase (Zucchi 2007, Olden 2007, Olden 2008, Olden 2009, San Marchi 2007, Elhoud 2010). The hydrogen-assisted fracture surfaces generally consisted of multifacets and riverlike patterns were commonly observed on each facet (Olden 2009, San Marchi 2007). Therefore, it was considered that the formation of cleavage microcracks in ferrite phase is the first step of hydrogen-assisted fracture in duplex stainless steels, and then the cleavage microcracks in ferrite phase are linked by more ductile fracture in austenite phase (Zucchi 2007, Olden 2007, Olden 2008, Olden 2009, San Marchi 2007, Elhoud 2010). Olden et al. (2008, 2009) stated that hydrogen-enhanced decohesion model (HEDE) rules fracture in ferrite phase and hydrogen-enhanced local plasticity model (HELP) is the main fracture mechanism in austenite phase. San Marchi et al. (2007) proposed a model in which the microcracks in ferrite phase are formed by stress concentrations induced by HELP in the austenite phase. However, there is a paucity of direct experimental evidence for such local fracture mechanisms.

Scanning probe microscopy (SPM), including scanning tunneling microscopy (STM), atomic force microscopy (AFM) and magnetic force microscopy (MFM), is a well known tool for imaging the surface morphology and magnetic microstructure of materials at high resolution. Recently, the present authors and colleagues successfully applied these techniques to identify the micromechanisms for hydrogen-assisted fracture in stainless steels (Zhang 2010, Zhang 2011, An 2013).

In this study, we observe the micromorphology of the fracture surface and microcrack formation in hydrogen-precharged super duplex stainless steel tensile tested at room temperature in air, by combined SEM, STM, AFM and MFM.

## 2. EXPERIMENTAL

Super duplex stainless steel (25.22% Cr, 6.94% Ni, 0.46% Mn, 3.9% Mo, 0.287% N, 0.011% C, 0.25% Si, 0.019% P, and 0.0006% S) with a nominal phase distribution of 50% austenite and 50% ferrite was used. The hydrogen-precharging and the tensile testing were carried out by San Marchi et al. in Sandia National Lab. The tensile specimens were thermally hydrogen-precharged in 138 MPa hydrogen gas at 573 K in a pressure vessel for 10 days. Tensile testing was performed at room temperature in air with a strain rate of $\sim 10^{-3}$ $s^{-1}$. After tensile testing, hydrogen concentrations were measured from samples taken from the specimens away from deformation regions. The hydrogen concentration was in a range from 120 to 130 wppm. The details of tensile testing have been published by San Marchi et al. (2007).

The fractured tensile specimens were longitudinally sectioned and mounted in epoxy resins to reveal the area below the fracture surface. The longitudinal sections were ground with sandpaper and electropolished in a solution of 20% perchloric acid, 70% ethyl alcohol and 10% glycerin. The fracture surfaces and longitudinal sections of the specimens were analyzed by SEM, STM, AFM and MFM at room temperature. STM, AFM and MFM observations were conducted in air using a Nanoscope IIIa Multi-SPM. STM images were obtained in the constant current mode with the tip bias from 500 to 800 mV and the tunneling current from 0.3 to 0.5 nA. AFM and MFM images were obtained in the tapping/lift mode with a lift height of 100 nm. Both the specimen and the magnetically coated MFM probe were magnetized by a permanent magnet with a field of 3800 G prior to MFM and their polarity were set to be opposite.

## 3. RESULTS AND DISCUSSION

Figure 1 shows the SEM images taken from the fracture surface and longitudinal section near the fracture surface of the hydrogen-precharged specimen. The fracture surface of the hydrogen-precharged specimen consists of relatively flat quasi-brittle facets with riverlike patterns, as shown in Fig. 1(a), while that of the non-charged specimen shows classic ductile dimples (not shown here). The facets on the fracture surface of the hydrogen-precharged specimen are separated from neighboring facets by steep steps or slopes which show more ductile fracture features including dimples. Careful analysis of the facets indicate that many of the river patterns start from inclusions, as shown by arrows in Fig. 1(a), indicating the starting of quasi-brittle facets from inclusions. The longitudinal section of the hydrogen-precharged specimen also shows that the fracture surface consists of small facets, steep steps and slopes, and many microcracks are formed at the specimen surface and in the bulk near the fracture surface, as shown in Fig. 1(b).

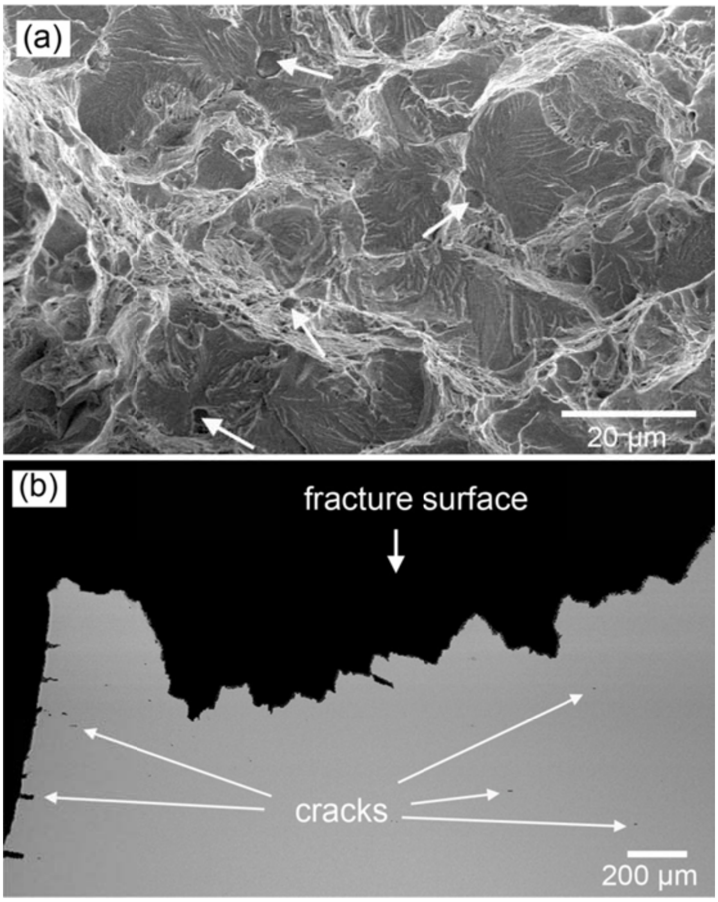


Fig. 1 SEM images of hydrogen-precharged super duplex stainless steel tensile tested at room temperature. (a) SEM image of the fracture surface. (b) SEM image of the longitudinal section near the fracture surface.

Figure 2 shows the MFM images taken from the longitudinal section of the hydrogen-precharged specimen. It is found that the microcracks formed at the surface and in the bulk initiate and grow in the ferrite phase but are stopped or deflected by the boundaries of the austenite phase, as shown in Fig. 2(a). The MFM image of the section of fracture surface also shows the small facets in the ferrite phase and the tearing traces in the austenite phase, as shown in Fig. 2(b). Therefore, the macroscopic mechanism for the hydrogen-assisted fracture in the duplex stainless steel, under our experimental condition, can be described as follows: the microcracks initiate and propagate in the ferrite phase and then link to each ether by tearing of austenite, as illustrated in Fig. 2(c). This is in agreement with previous reports (Zucchi 2007, Olden 2007-2009, San Marchi 2007, Elhoud 2010).

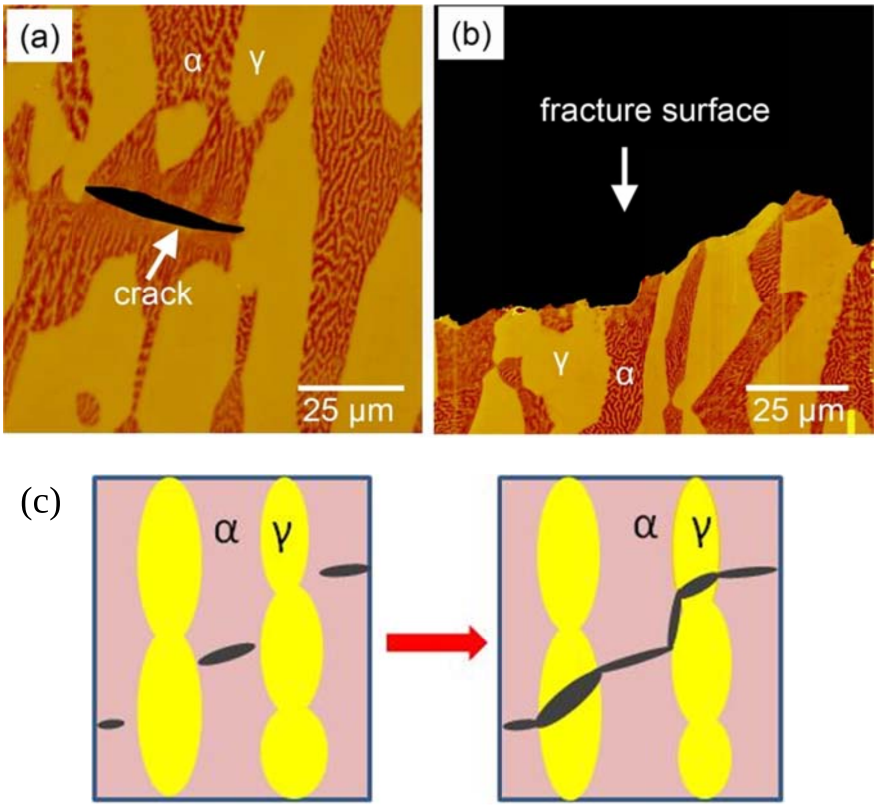


Fig. 2 MFM images of the longitudinal section of hydrogen-precharged super duplex stainless steel tensile tested at room temperature. (a) MFM image of a microcrack formed in the bulk. (b) MFM image of the section of fracture surface. (c) Illustration of macromechanism for hydrogen-assisted fracture in super duplex stainless steel.

In order to clarify the micromechanism of the quasi-brittle facet fracture in ferrite phase, we have observed the fracture surfaces by STM and found two typical surface patterns from the facet surfaces at nanoscale, an irregular particlelike pattern and a quasi-periodic corrugation pattern, as shown in Fig. 3. The irregular particlelike pattern seems to be nanoscale dimples with the diameter of about 40 nm and depth of about 5 nm, as shown in Fig 3(a), and the quasi-periodic corrugation seems to be plastic deformation trace with the periodicity of about 50 nm and the height less than 5 nm, as shown in Fig. 3(b). Recently, similar nanodimplelike patterns have also been observed from hydrogen-assisted quasi-brittle facets in ferritic pipeline steels, by Martin et al. (2011) and Neeraj et al. (2012) with high-resolution SEM, AFM and TEM. Neeraj et al. (2012) identified that such facet surfaces were covered with nanodimples and there were significant dislocation plasticity underneath the quasi-brittle facets. Then, they proposed nanovoid coalescence mechanism (NVM) based on plasticity-generated, hydrogen-stabilized vacancy damage and vacancy-induced nanovoid nucleation and coalescence.

The micromechanisms of the hydrogen-assisted cracking in duplex stainless steel have been discussed by Olden et al. (2007, 2008, 2009) and San Marchi et al. (2007). Olden et al. (2007, 2008, 2009) stated that HELP model controls the cracking in austenite phase but HEDE model dominates the cracking in ferrite phase. San Marchi et al. (2007) suggested that the stress concentration at phase boundary induced by hydrogen-enhanced local plasticity in austenite leads to the formation of cleavage microcrack in ferrite phase. However, our high-resolution observations by STM clearly reveal that the facet surface is covered with two typical patterns, the nanodimplelike pattern and quasi-periodic nanocorrugation pattern, which can be correlated with hydrogen-enhanced highly localized plastic deformation. Therefore, we can conclude that the hydrogen-assisted cracking in ferrite phase is not a cleavage fracture but a local ductile fracture controlled by the HELP-based cracking mechanism.

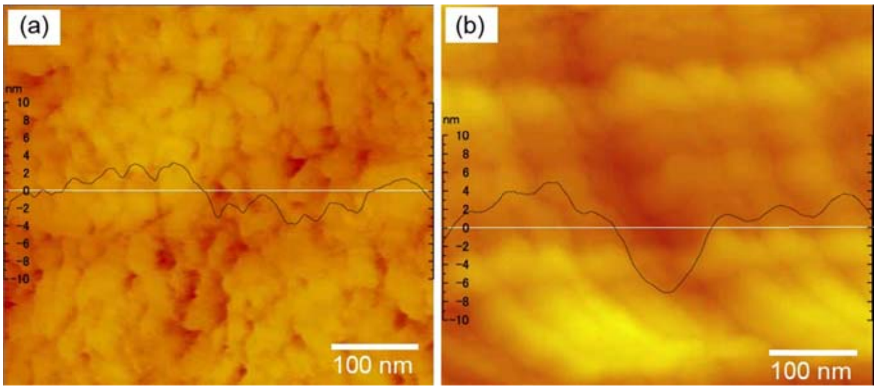


Fig. 3 STM images taken from the facets. (a) Nanoscale dimples. (b) Quasi-periodic corrugation. The inserts show the sectional profiles along the white lines.

## 3. CONCLUSIONS

SEM, STM, AFM and MFM have been applied to characterize the microstructure of fracture surface and microcrack formation in hydrogen-precharged super duplex stainless steel, and the following conclusions are obtained.
(1) The hydrogen-assisted microcracks preferentially initiate and grow in ferrite phase and are stopped or deflected by the boundaries of austenite phase. Then, the stepwise fracture occurs by tearing of austenite phase, resulting in the multifacets fracture.
(2) The facet surfaces exhibit two typical features at nanoscale, the nanodimplelike patterns and quasi-periodic nanocorrugation patterns that can be correlated with hydrogen-enhanced highly localized plastic deformation. Therefore, the HELP-based cracking mechanism rules the hydrogen-assisted fracture in both the ferrite phase and austenite phase.

## REFERENCES

Marrow, T.J., Hippsley, C.A. and King, J. E. (1991), “Effect of mean stress on hydrogen assisted fatigue crack propagation in duplex stainless steel”, *Acta Metall. Mater.* **39** (6), 1367-1376.

Zheng, W. and Hardie, D. (1991), “The effect of hydrogen on the fracture of a commercial duplex stainless steel”, *Corrosion Science* **32** (1) 23-36.

Zucchi, F., Grassi, V., Monticelli, C. and Trabanelli, G. (2006), “Hydrogen embrittlement of duplex stainless steel under cathodic protection in acidic artificial sea water in the presence of sulphide ions”, *Corrosion Science* **48** (2), 522-530.

Olden, V., Thaulow, C., Johnsen, R. and Østby, E. (2007), “Cohesive zone modeling of hydrogen-induced stress cracking in 25% Cr duplex stainless steel”, *Scr. Mater.* **57** (7), 615-618.

Olden, V., Thaulow, C., Johnsen, R., Østby, E. and Berstad, T. (2008), “Application of hydrogen influenced cohesive laws in the prediction of hydrogen induced stress cracking in 25% Cr duplex stainless steel”, *Eng. Fract. Mech.* **75** (8), 2333-2351.

Olden, V., Thaulow, C., Johnsen, R., Østby, E. and Berstad, T. (2009), “Influence of hydrogen from cathodic protection on the fracture susceptibility of 25%Cr duplex stainless steel-Constant load SENT testing and FE-modelling using hydrogen influenced cohesive zone elements”, *Eng.Fract. Mech.* **76**, (7), 827-844.

San Marchi, C., Somerday, B.P., Zelinski, J., Tang, X. and Schiroky, G.H. (2007), “Mechanical Properties of super duplex stainless steel 2507 after gas phase thermal precharging with hydrogen”, *Metall. Mater. Trans. A* **38** (11), 2763-2775.

Elhoud, A.M., Renton, N.C. and Deans, W.F. (2010), “Hydrogen embrittlement of super duplex stainless steel in acid solution”, *Int. J. Hydrogen Energy* **35** (12), 6455-6464.

Zhang, L., An, B., Fukuyama, S., Iijima, T. and Yokogawa, K. (2010), Characterization of hydrogen-induced crack initiation in metastable austenitic stainless steels during deformation, *J. Appl. Phys.* **108** (6), 063526.

Zhang, L., An, B., Iijima, T., Fukuyama, S. and Yokogawa, K. (2011), “Anomalous plastic deformation and martensitic transformation in metastable austenitic steels at low strain rate characterized by in-situ hydrogen and argon releases and scanning probe microscopy”, *J. Appl. Phys.* **110** (3), 033540.

An, B., Itouga, H., Iijima, T., San Marchi, C. and Somerday, S.P. (2013), “Hydrogen-assisted twin boundary fracture of type 304 austenitic stainless steel at low temperature investigated by scanning probe microscopy”, Proceedings of the ASME2013 Pressure Vessels & Piping Conference, PVP2013-97355, Paris, France, July 14-18.

Martin, M., Fenske, J.A., Liu, G.S., Sofronis, P. and Robertson, I.M. (2011), “On the formation and nature of quasi-cleavage fracture surfaces in hydrogen embrittled steels”, *Acta Mater.* **59** (4), 1601-1606.

Neeraj, T., Srinivasan, R. and Li, J. (2012), “Hydrogen embrittlement of ferritic steels: Observations on deformation microstructure, nanoscale dimples and failure by nanovoiding”, *Acta Mater*. **60** (13), 5160-5171.